

Abstract

We introduce methods for visualization of data structured along trees, especially hierarchically structured collections of time series. To this end, we identify questions that often emerge when working with hierarchical data and provide an R package to simplify their investigation. Our key contribution is the adaptation of the visualization principles of focus-plus-context and linking to the study of tree-structured data.

Our motivating application is to the analysis of microbial time series, where an evolutionary tree relating microbes is available a priori. However, we have identified common problem types where, if a tree is not directly available, it can be constructed from data and then studied using our techniques. We perform detailed case studies to describe the alternative use cases, interpretations, and utility of the proposed visualization methods.

Keywords: D3, focus-plus-context, linking, time-series, tree-structured, R

*This research was supported in part by an NIH training grant (5T32GM096982-03).

†This research was supported in part by NIH grant R01 AI112401.

0.1 Introduction

We introduce methods for visualization of data structured along trees, especially hierarchically structured collections of time series. We hope both to characterize generically useful techniques for interactively visualizing hierarchical data and to offer practical tools for implementing such displays. To this end, we identify questions that often emerge when working with hierarchical data and provide an R package to simplify their investigation (Ihaka and Gentleman 1996).

Our key contribution is the adaptation of the visualization principles of focus-plus-context and linking to the study of tree-structured data (Buja, Cook, and Swayne 1996, Becker and Cleveland (1987)). Our motivating application is to the analysis of bacterial time series, where an evolutionary tree relating bacteria is available a priori. However, we have identified common problem types where, if a tree is not directly available, it can be constructed from data and then studied using our techniques.

We have implemented our visualizations in D3, but encapsulated in an R package, called `treelapse`, to facilitate rapid turnover from data preparation and modeling to interactive exploration, and vice versa. Our code is open-source, and available at <https://github.com/krisrs1128/treelapse>¹. We hope this package encourages data analysts to work at the border between data modeling and visualization, and more generally empowers a wider audience to apply less widely known, but powerful, visualization ideas.

The paper is organized as follows. First, we describe our motivating application to the microbiome and the associated generic analysis tasks. Next, we review the underlying visualization principles behind our contributions. Then we then connect these principles to analysis tasks we identified earlier, describing in detail the visualization methods we have implemented in `treelapse`. We close with several case studies using publicly available data across both microbiome and non-microbiome related applications.

0.1.1 Problem Motivation

A microbiome is a community of bacteria living in given environments, for example, ocean water or the human gut (Consortium and others 2012, Consortium and others (2012), Cho and Blaser (2012)). Progress in the field has been rapidly accelerated by the advent of genomic technologies, which enable detailed quantification of bacterial ecological structure and its influence in human and environmental health. Being concerned with both bacterial community structure and human health, the field exists at the border between ecology and medicine; consequently, papers in the area often apply a blend of exploratory data analysis and formal statistical inference.

The two essential microbiome analysis problems that motivated our work are the tree-structured differential

¹Link removed in blinded manuscript, but available to editor.

abundance and differential dynamics problems. In the differential abundance problem, we attempt to compare the abundances of individual bacteria across experimental conditions – for example, treatment vs. control or healthy vs. diseased. This is the microbiome analog of differential expression analysis in genomics (Anders and Huber 2010). We prepend the description “tree-structured” because, in practice, researchers generate interpretations about intermediate taxonomic orders – it is more interesting to discover novel behavior taxonomic levels between high-order phyla and low-level species. Hence, we frame the tree-structured differential abundance problem as the question of identifying the largest taxonomic subtree whose associated bacteria are differentially abundant.

In the tree-structured bacterial dynamics problem, the goal is to describe changes in bacterial abundances in an environment over time. As in the differential abundance problem, it is useful if these descriptions can be given at the highest subtree at which the pattern appears. Specific questions of interest often have an ecological flavor. For example, researchers are often interested in understanding how bacterial populations respond to sudden or gradual environmental changes or how species fill, drop out from, or compete for environmental niches. Medically, these questions are important for illuminating the impact of antibiotic time courses or diet changes, for example.

0.1.2 Problem Abstraction

To unify the tree-structured differential abundance and bacterial dynamics problems, we identify the data with a collection of random variables indexed by nodes in a prespecified tree structure. In the differential abundance problem, each random variable lives in \mathbb{R}^G where G is the number of groups being compared. Each coordinate represents the abundance for that group, and a node exhibits differential abundance when the coordinates are drawn from different distributions. On the other hand, in the bacterial dynamics problem, each random variable is a time series, living in \mathbb{R}^T .

In both of these applications, we constrain the values of parent nodes according to the value of the children nodes: we define the value at each node to be either the sum or average of all descendant tips. However, it is possible to imagine situations where the internal nodes are drawn from their own distribution, unconstrained by descendants. In general, analysis in this abstraction focuses on describing the distribution of these random variables as a function of their position across subsets of the tree. The essential difficulty in these problems is high-dimensionality – there are many tree nodes, each holding a vector-valued random variable. Even simply navigating across the tree and comparing coordinates in the observed variables is a challenge; ideally we could construct a succinct representation of the essential covariation across subtrees and coordinates.

This framework suggests other potential application areas, not all of which have a priori known tree

structures. For example, collections of spatially-indexed time series are frequently encountered in practice – consider energy consumption, product sales, or high school dropout rates across regional districts. This type of data has an implicit tree structure – at the top level are different states, while at the bottom are individual census tracts, say. Analysis here revolves around the question of how variation across time series is related to their geographic position. A case study to this type of data is given in Section 0.4.3.

Alternatively, if this type of hierarchical contextual information is not directly available, a tree structure can be learned from the data. This could be achieved by learning a hierarchical clustering on the original series. Further, if contextual information is available, but it is not hierarchical, it is possible to setup a supervised problem that uses context to predict features of the time series. We can construct a tree by applying a tree-based classifier (Breiman et al. 1984) or extracting a regression tree from a more complex supervised model (Boz 2002, Saito and Nakano (2002)). Analysis then focuses on how different partitions of the contextual, covariate space relate to observed time series. This approach is described in Section 0.4.4.

Finally, note that, while we have focused on time series valued nodes, all of this discussion could be translated to studying high-dimensional data via parallel coordinates (Inselberg and Dimsdale 1991). The usual parallel coordinates challenges remain, mainly selecting scales for and ordering across the different coordinates, but the linking and focus-plus-context can still be employed this setting.

0.2 Background Literature and Solution Principles

Now that we have specified the essential questions of interest, we survey some ideas from the visualization literature that can be applied to answer them. As the core difficulty is high-dimensionality, so it should be no surprise that the techniques we adapt come from the literature on high-dimensional data visualization, namely, focus-plus-context and linking.

The focus-plus-context principle is that large collections of visual elements can be studied at multiple scales, by simultaneously focusing" on a few elements of interest and maintaining the “context” of the coarser-scale background. A simple example of this idea is to include a search box that highlights matching samples (focus) and mutes the rest (context). Two more sophisticated methods anchored in this idea are timeboxes and Degree-of-Interest (DOI) trees; both are central to the proposals in treelapse (Hochheiser and Shneiderman 2004, Heer and Card (2004)). In timeboxes, a collection of time series are graphically queried using interactive brushes. Series that pass through all of the user-specified brushes are highlighted, and the rest are faded to the background. Hence, time series meeting the constraints imposed by the brushes are focused, while the remainder are de-emphasized, though they remain present as context. This method can be interpreted programmatically as the visual analog of a database query, or probabilistically as the conditional distribution for the full series, given it passes through certain bounds.

In DOI trees, the viewer’s attention is focused on a collection of high-interest nodes, while the remaining lower-interest nodes are left on the fringes as context. The implementation is modularized into two tasks – the determination of a DOI distribution over nodes in the tree and visual layout of a tree given DOI assignments. The DOI distribution used in (Heer and Card 2004) places maximal interest on the node that the user had most recently clicked, along with all ancestors. The DOI for all other nodes is defined as the distance to the closest maximal interest node. The layout step then trims low-interest subtrees until the remaining nodes fit within a given screen size. By adjusting the minimal DOI below which nodes are hidden, the user can transition between node-specific and full-tree scales.

In linking, alternative representations of the same samples are placed side-by-side in order to display covariation across views. A canonical application is to linked scatterplot brushing (Becker and Cleveland 1987). Here, a scatterplot matrix gives the relationship between all pairs of variables. Points brushed in one scatterplot are then highlighted in all others. For example, this helps the user determine whether an outlier in one dimension is an outlier in others. Another instance of this idea links the results of dimensionality reduction methods to displays of the raw data, as implemented by XGobi and Cranvas, for example (Xie et al. 2013, Swayne, Cook, and Buja (1998)). As in timeboxes, linking can be interpreted as database queries or conditional probabilities: given a subset of the series after conditioning on the values for one set of features, what are the values for a second set (Buja, Cook, and Swayne 1996)?

Finally, unrelated to established visualization principles, we note that our work is deliberately grounded in the R software ecosystem. This connection is made using the `htmlwidgets` package (Vaidyanathan et al. 2014). Not only does linking R with D3 make these visualization methods more broadly accessible, we hope to facilitate exchange between data modeling and interactive visualization. Moreover, our tools are intentionally limited in scope – designed to facilitate this dialog for a specific class of problems, rather than providing a toolbox for generic types of visualization design. We believe that this narrow context within a broad ecosystem strikes a balance between problem-specificity and ease-of-use.

0.3 Specific Proposals

Our first proposed visualization technique is a minor modification of the DOI tree. The standard DOI tree definition does not have any notion of data defined at nodes, it is only used a device for navigating tree structures. A trivial extension can encode scalar data at nodes: have the node radius reflect the associated scalar value. To reinforce this effect, we can adjust the width of the parent edge. When parent nodes have values equal to the sum of their children, this creates the effect of values “flowing” from the root to leaves. To help viewers make use of their domain knowledge, we have included a search box that highlights paths to nodes with matching terms. Edges are ordered from widest on the left to narrowest on the right. While this method can only represent a single scalar-value per tree node, it suggests an approach to the

tree-structured differential abundance problem, which we call the DOI sankey.

In the DOI sankey, we split each edge in the DOI Tree across different groups. For example, suppose we have the average counts for treatment and control groups at each tree node. Every edge in the tree is split into two colors², with relative widths of the different colors reflecting differences in sizes for the two groups. The overall width of each edge represents the sum of values across all groups.

This display is designed to facilitate investigation of the tree structured differential abundance question. For example, for a single node and a single group, first compute the average abundance at that node among all samples in that group. This will give the width for that group’s color on the edge leading to the specified node. Differentially abundant subtrees then correspond to subtrees where some colors occupy more space than others. That is, this representation makes it easier to identify points where the “flows” for different groups diverge – the colors begin to separate. The DOI principle assists navigation across the tree structure, allowing focus on individual flow structures without losing broader tree context.

Our third display is directed at the bacterial dynamics question. Here, two panels are arranged one over the other; one displays all time series, while the other displays all tree nodes, with node sizes reflecting the time series value at that node. For this reason, we call the display, Timebox Trees. In the time series panel, we have directly implemented the timeboxes idea. We then link the panels: when a set of series is highlighted by the timeboxes, the associated tree nodes are also highlighted. For example, timeboxes can be used to focus on a set of series with specific shape – increased abundance after an ecological shock, for example – and identify along what subtrees this pattern is present. To further focus on specific elements, a pan-zoom scented widget is provided (Willett, Heer, and Agrawala 2007). The widget is a miniature version of the full time series panel, equipped with a single brush whose extent specifies the limits in the main time series panel. As in the DOI trees and sankeys, a search bar can be used to highlight those series of interest a priori.

The final display currently implemented in the package is the natural converse of the timebox trees display. Rather than defining visual queries in terms of time series, it defines queries using nodes in the tree. For this reason, we call the display Treeboxes. Rather than focusing on the intersection of brushes, as in timebox trees, we focus on the union of brushed over nodes. This allows us to highlight series associated with nodes on distant subtrees. This display is also suited for the bacterial dynamics problem. For example, by highlighting all nodes at one taxonomic level in the tree, we can easily summarize the time series pattern for all the taxa at that level. Alternatively, focusing on all the children below a single node makes it possible to see how much correlation and competition there is between taxonomically similar bacteria. As in the timebox trees display, a search box and pan-zoom scented widget are provided.

²We use the colorbrewer palette to facilitate readability (Brewer, Hatchard, and Harrower 2003)

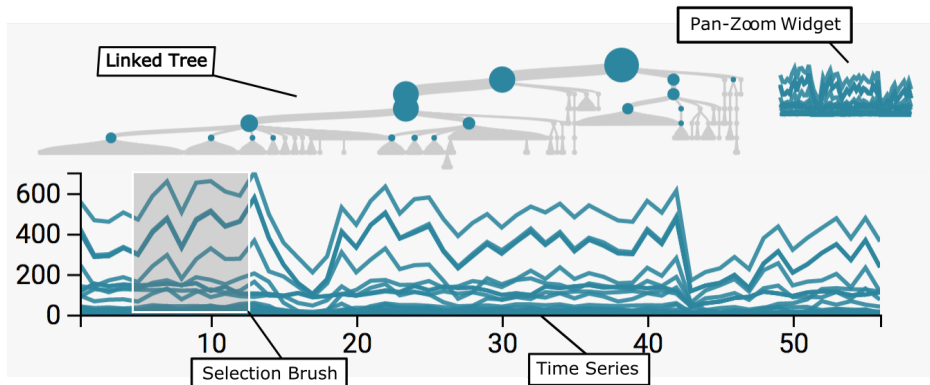


Figure 1: The two antibiotic time courses are readily apparent even when only highlighting the most abundant taxa. We have annotated the figure with its three main components.

0.4 Case Studies

We now delve into applications on real data. Our goals are to illustrate potential workflows that incorporate treelapse, describe the formulation of questions that can be naturally investigated with our methods, and provide example interpretations on treelapse output. Our examples are also chosen to reflect the range of problem domains to which the package can be applied – though it was motivated by applications to the microbiome, it is not tied to it. More importantly, we argue that the visualization principles reviewed above can substantively improve the practice of data analysis in the class of problems to which we have limited ourselves.

0.4.1 Bacterial Dynamics of Antibiotics Time Courses

(Dethlefsen et al. 2008) investigates the effect of antibiotics on bacterial community composition from an ecological perspective. The study tracks the microbiome of three patients across ten months, with two five-day antibiotic time courses separated by 6 months. Discerning the variation in resilience across bacteria is important, considering the the role of bacteria in health and not just disease.

We approach the data using the linked time and treebox views, after first filtering low variance taxa and taking an asinh transformation. An initial view, Figure 1, reveals two dramatic drops in the overall bacterial abundance time series during the antibiotics time courses. Two more subtle effects are also suggested from this view,

- The second antibiotic treatment seems to have a more lasting effect, as the series take longer to return to their original values.
- Some high level taxa appear relatively unaffected by the first antibiotic treatment. By more closely inspecting the display, we are able to identify these as members of the Bacteroidetes phylum, see Figure 2.

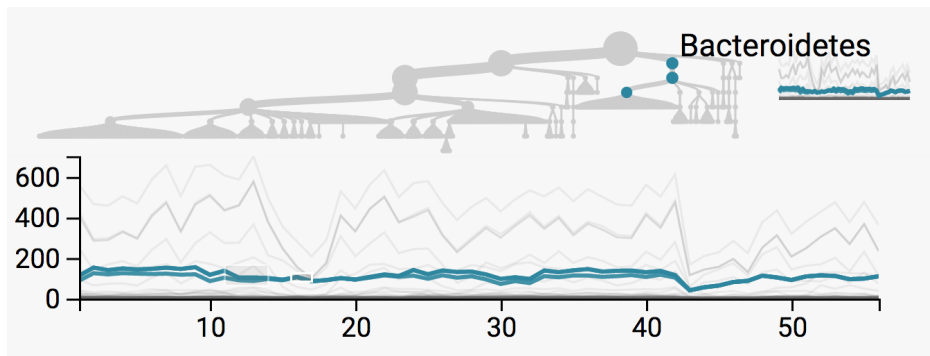


Figure 2: Introducing a second box into the timebox display identifies the Bacteroidaceae as a taxon only mildly impacted by antibiotics.

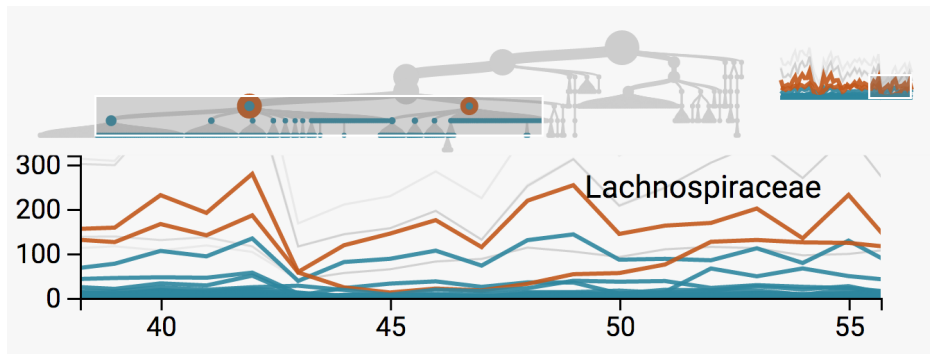


Figure 3: Zooming into the second antibiotic timecourse and highlighting the Lachnospiraceae and Ruminococcus, we see that the Ruminococcus took more time to recover to pre-treatment levels.

Next, using the scented widget, we focus on the window around the second antibiotic treatment. We apply the treebox display to compare then behavior of different families of Firmicutes, Lachnospiraceae and Ruminococcus. We suspect that these taxa are associated with the delayed recovery after the second time course. To investigate this, we input these family names in the search box to isolate their positions on the tree; then we apply brushes to highlight the series that contribute to these higher-level families. The resulting view is given by Figure 3

Alternatively, we can summarize each node by the average across its descendants – this brings attention to individual bacteria that may be underlying some of the broader taxonomic patterns we have noted when studying the subtree sums. For example, in Figure 4, we highlight all families below order Ruminococcus, suggesting that the decrease due to antibiotics occurs uniformly across almost all families. A point that was not evident in the earlier sum-across-descendants view is that, after the second treatment of antibiotics, a few of the Ruminococcus families recover more rapidly than the rest, for example the Unc095d3 (highlighted in red) are only briefly affected. In contrast, most families seem to recover in unison after the first treatment. Further, note that in this subtree averages view, the tree display has changed. This is because, at each branching point, we place the node with larger average value on the left. This places the Verrucomicrobiae

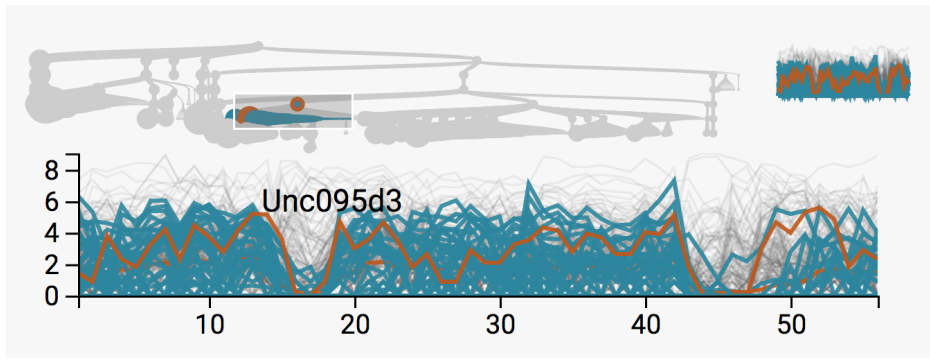


Figure 4: By hovering over the *Ruminococcus* branches, we see that there is a prolonged effect of the antibiotics time courses more or less uniformly across the lower taxonomic orders.

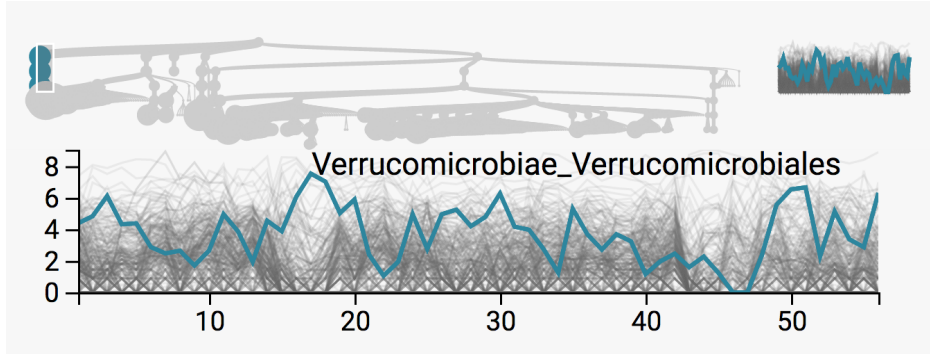


Figure 5: The subtree averages aggregation brings attention to the Verrucomicrobiae, which though only present as a few species, are each rather abundant. In particular, they seem to increase after the first antibiotic time course.

at the far left, which seem to have large abundance over many time points. This phylum had been previously obfuscated – because there are not many leaves associated with this phylum, the sum was small. Interestingly, the abundance of these bacteria seems to *increase* after the first antibiotics treatment. Be cautious, however, that the average over only a few Verrucomicrobiae species will be a more variable estimate than the averages over the more prevalent phyla.

0.4.2 Differential Bacterial Abundance and Preterm Births

The study (DiGiulio et al. 2015) tracked the abundance of bacteria in the vaginal microbiome during pregnancy in an effort to study relationships between bacterial community composition and preterm birth. Ideally, it would be possible to develop clear bacterial signatures associated with preterm births.

Unlike the antibiotics study, we have measurements across more individuals than we could reasonably inspect one at a time. While we could average across all individuals, we will take our cue from (DiGiulio et al. 2015) and place each sample into one of five Community State Types (CSTs), identified via k-medoids. In that study, a linear model identified one of these CSTs (CST 4) as significantly more diverse, further it

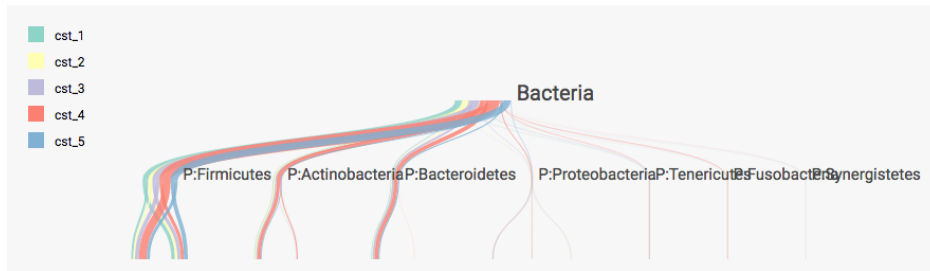


Figure 6: The increased diversity among samples in CST 4 is represented by the relatively larger contribution of red edges to branches outside of the Firmicutes.

appeared associated with preterm births. Here, we corroborate this finding using exploratory views.

Therefore, our focus here is on the differential abundance question, rather than dynamics. We would like to provide visual representations of differential abundance across CSTs and also between preterm and non-preterm births. (DiGiulio et al. 2015) interpreted the CSTs using a heatmap, with bacteria ordered according to a hierarchical clustering. By using the DOI sankey instead, we can interpret the CSTs in their taxonomic context and at multiple scales of taxonomic resolution. Further, while (DiGiulio et al. 2015) focused on identifying associations between preterm births and CSTs – presumably because testing individual bacteria loses power – we can compare bacterial abundances between preterm and non-preterm samples along subtrees, without requiring CSTs as an intermediary.

In Figure 6, we compare the 5 CSTs according to their values along the subtree. Specifically, we took the average of all samples within each CST to define values at the (species-level) leaf nodes, and then aggregated the averages up to the root. It is immediately clear that samples from CST 4 have much more taxonomic diversity. Further, focusing on the Lactobacillaceae family, we note that the differential abundance of these bacteria distinguishes the remaining CSTs, see Figure 7.

Alternatively, in Figure 6, we avoid working with CSTs, displaying instead averages among samples associated with either preterm or term births. The green edges are associated with preterm births – we see that they contribute more weight to phyla outside the Firmicutes. This is consistent with the claim that CST 4, the most diverse of the CSTs, is associated with preterm births.

0.4.3 Dynamics in Housing Prices

We next consider an application unrelated to the microbiome, but with relatively clear hierarchical structure. Our data are downloaded from Zillow³, and give the Zillow Home Value Indexes at the neighborhood level, across the country, computed monthly between 1996 and 2016. In our display, we have taken the base 10 log of these indexes. As our hierarchical structure, we use each neighborhood’s assignment to state,

³<http://www.zillow.com/research/data/>

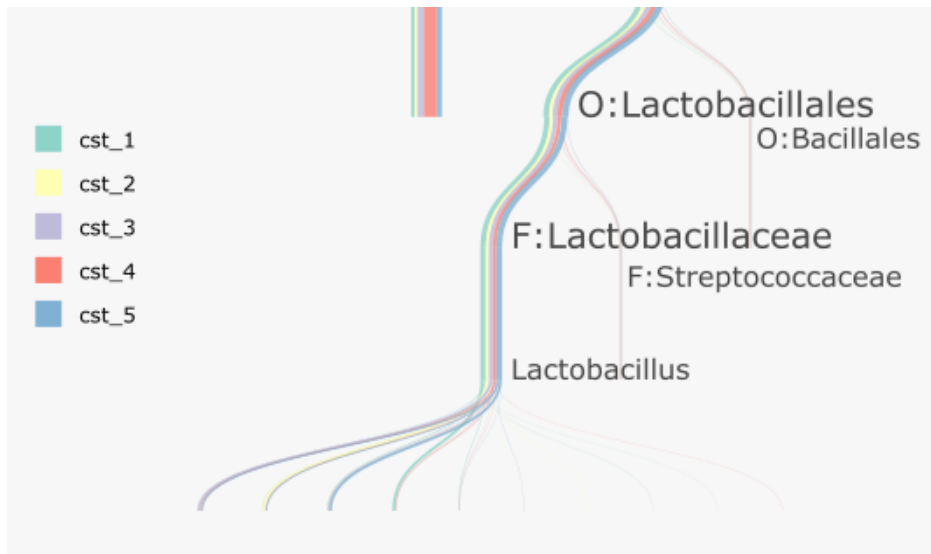


Figure 7: Zooming into the Lactobacillaceae family, we notice that the difference between the remaining four CSTs is related to which types of Lactobacillus are most prominent.

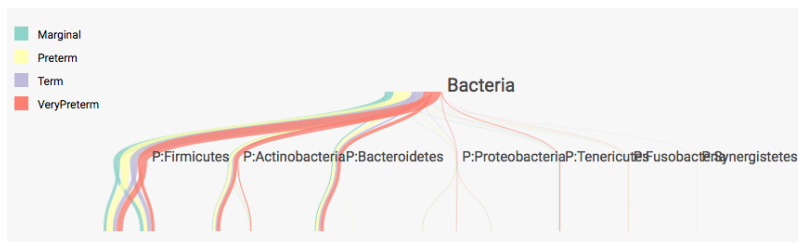


Figure 8: Samples with high levels of phyla other than Firmicutes appear to be related to preterm births.

regional, county, and city levels. We represent each of these coarser spatial categories using the average of all neighborhoods contained in them. We have filtered down to the 890 neighborhoods in California; rendering more neighborhoods while keeping all 246 timepoints causes the interface to lag⁴.

Our basic analysis revolves around geographic and temporal variation in home prices. We are especially interested in the effect of the 2008 recession and any variation in the lead-up to or recovery from this event. These questions can be naturally framed using timebox trees and treeboxes.

We first study variation in prices at the city level. These series can be highlighted using a single brush in treeboxes, since each spatial level is displayed at the same height in the tree. The resulting display is given in Figure 9. From a high level, the housing bubble, decrease in prices due to the recession, and subsequent recovery are readily apparent. The city-level view makes it clear that not all neighborhoods were equally affected by the recession – richer cities plateaued at their 2008 prices, middle-income cities saw moderate decreases, and poorer cities saw the most significant declines in home prices. These more significant declines tended to occur in cities that had recently seen rapid increases during the housing bubble. Finally, we note that the range in home prices seems to have increased after the recession, speaking to the differential long-term effect of the recession on prices.

Alternatively, we can study the trajectories of home prices among neighborhoods, conditional on their being middle-income before the recession. We generate the sequence of views in Figures 10, 11, and 12 to this end. The first of these figures isolates neighborhoods with middle incomes before the recession, using a single timebox. Since there appears to be a divergence in trajectories after the recession, we introduce a second post-recession timebox, dragging it over series with higher and lower incomes during this second time period. This is the content of Figures 11 and 12. Inspecting the highlighted tree nodes associated with these series, we find that most of the middle-income series that increased after the recession are associated with middle-income neighborhoods within the coastal Southern California counties. In contrast, those middle income series that saw decreases were mostly located in Central California and Oakland.

The previous analysis highlights the fact that, within even narrow geographic regions, there can be substantial variation in prices. We can study this directly using treeboxes. In Figure 13 we have highlighted all series in San Francisco County. We see that, in 2016, prices range from around $10^{5.6} \approx \$400,000$ to $10^{6.7} \approx \$5$ million. So, while all these neighborhoods tend to be among the more expensive ones in California, prices can vary in a non-smooth way across geographic space.

We conclude this example with a caveat that the Zillow data are not representative of all neighborhoods in California, only those with enough listings on the site, so should be supplemented by other data sources for any substantial decision-making.

⁴See Section 0.5 for potential optimizations, however.

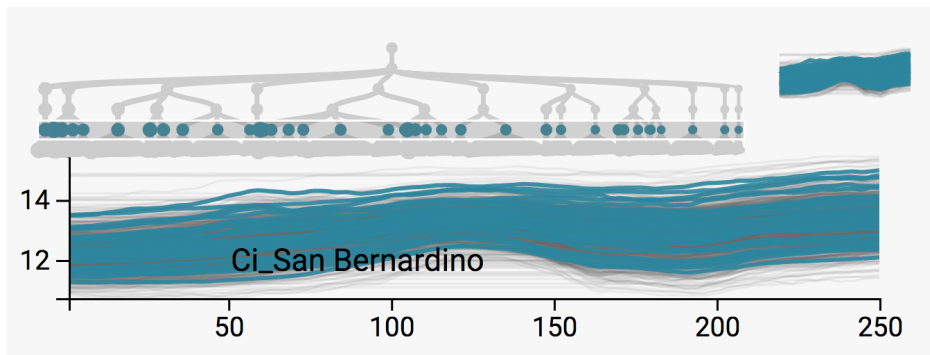


Figure 9: California home prices at the city level, between 1996 and 2016. The effect of the 2008 recession is clear, and we have hovered over the San Bernardino series, to display the identity of one of the cities most strongly affected by the recession.

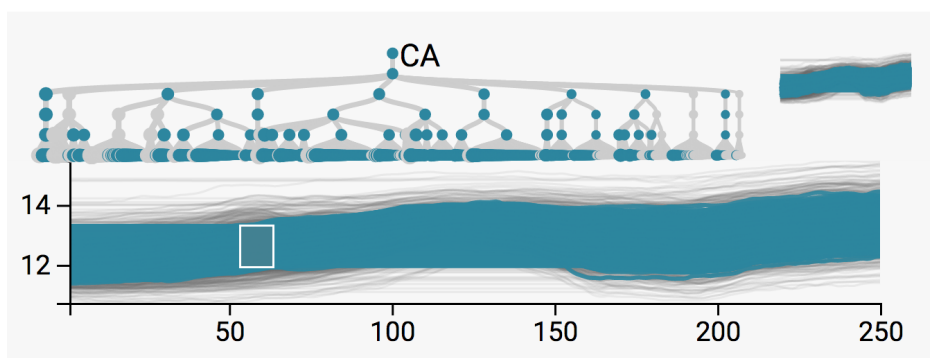


Figure 10: Neighborhoods with mid-range home prices before the recession are selected here. Note that the collection of series seems to widen after 2008 – we are interested in whether there are reliable predictors of these alternate trajectories, given their similar starting points.

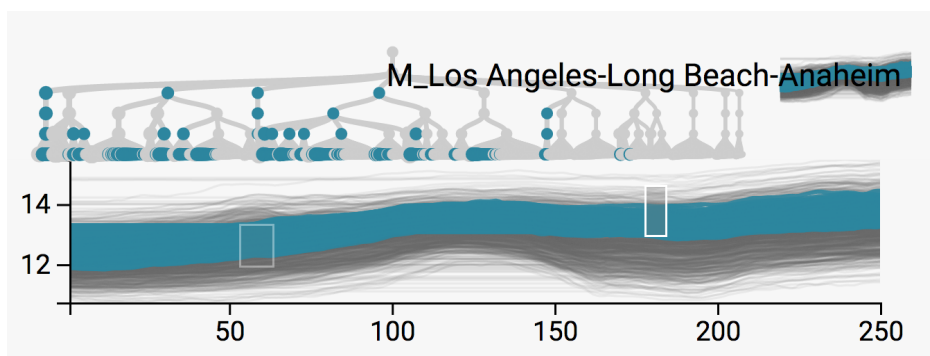


Figure 11: Among those neighborhoods with mid-range prices before the recession, we have selected those that recovered more rapidly. These appear to be located mainly in Los Angeles and San Diego counties.

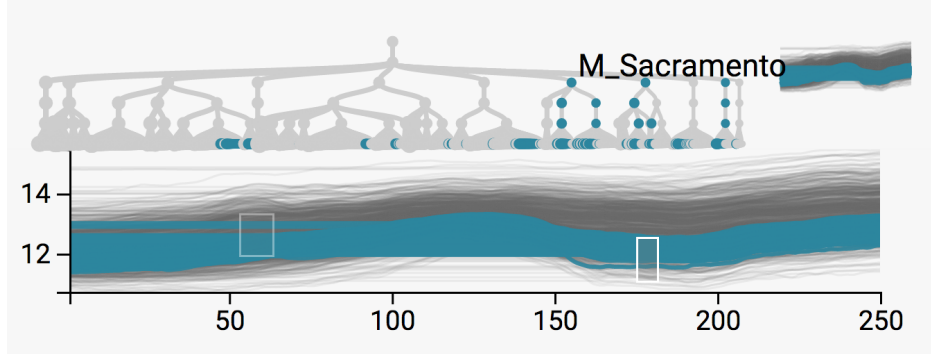


Figure 12: Rather than selecting mid-range series that recovered quickly, we can isolate those whose prices remained depressed after the recession. These seem mostly to be located in Central California and the East San Francisco Bay Area.

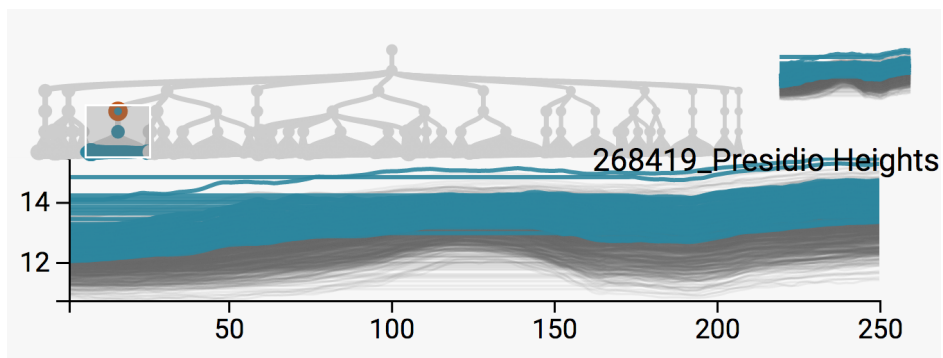


Figure 13: To study the range in home prices within San Francisco County, we can select the associated nodes using a treebox.

0.4.4 Sources of Variation in Bikesharing Demand

Our next example is a study in bikesharing demand, included as an example of analyzing collections of time series when there is no obvious hierarchical structure a priori. The data are available at the UCI Repository⁵ and were originally collected by a Washington D.C.-based bikesharing system for use in a Kaggle prediction competition. The data are hourly measurements of bike demand, aggregated across all bikesharing stations, over two years, along with supplemental weather data. In the competition, participants were asked to predict the hourly demand on a held-out test set. Here, we adopt a descriptive view instead, attempting to characterize factors associated with variation in bikesharing demand.

Like the Zillow home prices application, we study this problem as one of describing a large collection of related time series. Here, we consider the demand during a single day to be one time series; this is a natural choice considering the daily periodicity of bike demand. To arrange these daily series along an interpretable tree structure, we apply a regression tree relating the supplemental data to the bikesharing demand (Breiman et al. 1984). In more detail, we built this tree by noting the “two table” structure of this problem: one describes bike demand, the other holds the supplemental data. In both, the rows index days, while the columns index either hours or supplemental features. Our tree is the trained regression tree after predicting demand at 8AM based on the supplemental data. We choose this response because (1) we need a univariate response in order to apply regression trees and (2) the more straightforward reduction to daily-average-demand fails to distinguish between weekdays and weekends, whose series appear qualitatively very different from each other.

Given this response, the first split in the regression tree is (unsurprisingly) the difference between weekends and weekdays. This is emphasized in Figures 14 and 15, respectively; using timeboxes to isolate the two types of series highlight the left and right sides of the tree, respectively. For a more subtle effect, we select the internal nodes associated with the first split below the weekday vs. weekend split; these are given in Figures 16 and 17. This suggests that weekday demand increased during the second year.

In contrast to these general questions about daily demand, we could ask a more granular question about specific time windows. For example, what characterizes days on which there is larger than average demand after midnight? We can select these series after first zooming into this time window. Figure 18 reveals that the highlighted series are associated with the warm-weekend split, which seems quite reasonable in retrospect.

Finally, we can study the behavior of the regression tree itself using the DOI sankey. Here, we group samples according to their quintile of 8AM demand and then count the abundance of the groups flowing down different branches. We find that the quintiles are each rather strongly separated after descending

⁵<https://archive.ics.uci.edu/ml/datasets/Bike+Sharing+Dataset>

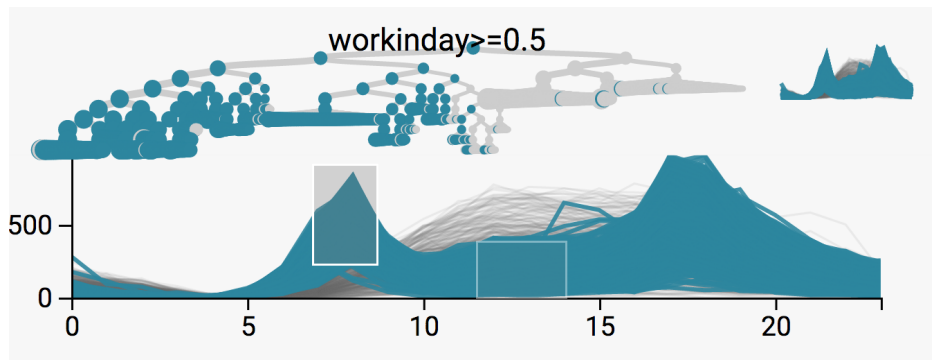


Figure 14: The two peaks at rush hour distinguish weekday series from the rest.

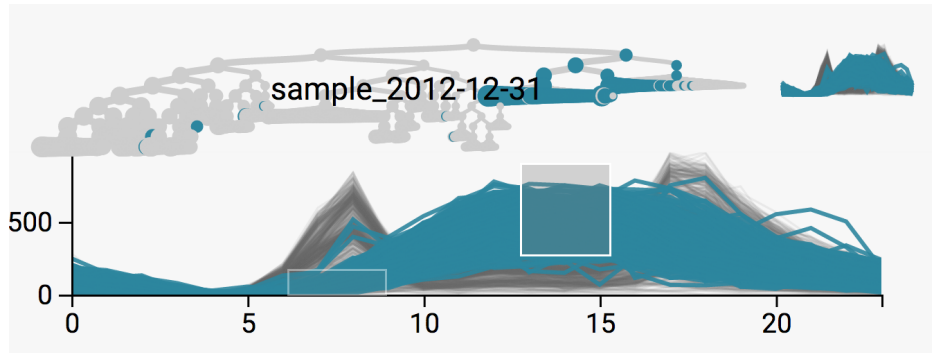


Figure 15: Unlike weekday demand, weekend demand is unimodal. The few weekday series with unimodal series seem to be associated with holidays. This is the case for New Years' Eve, which is currently hovered over in the tree.

even a few steps down the regression tree – for example, Figures 16 and 17 focus on 2011 vs. 2012 split among weekday samples, showing that this split distinguishes between samples falling in the second and third quintiles of 8AM demand.

This interactive representation of regression trees is potentially more useful on larger trees that cannot be easily parsed in a single view; in this sense the bikesharing tree is relatively simple. In our ideal data analysis workflow, we imagine the analyst applying interactive visualization and modeling techniques in an iterative, nonlinear fashion.

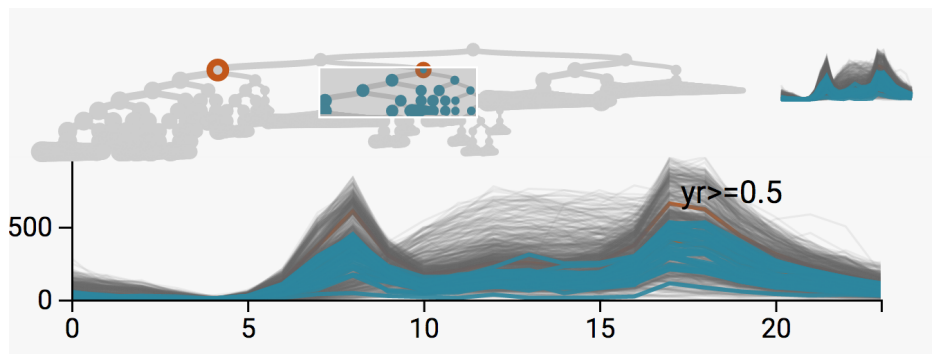


Figure 16: Weekday demand appears larger in 2012 than 2011 – compare with the next figure.

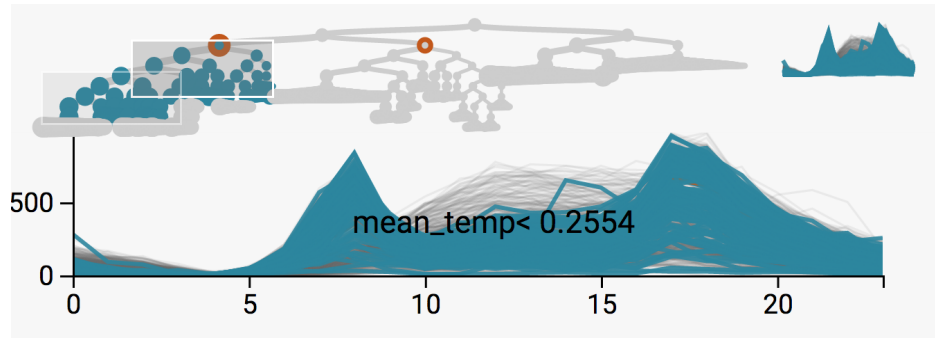


Figure 17: Weekday demand increased in 2012 – compare with the previous figure.

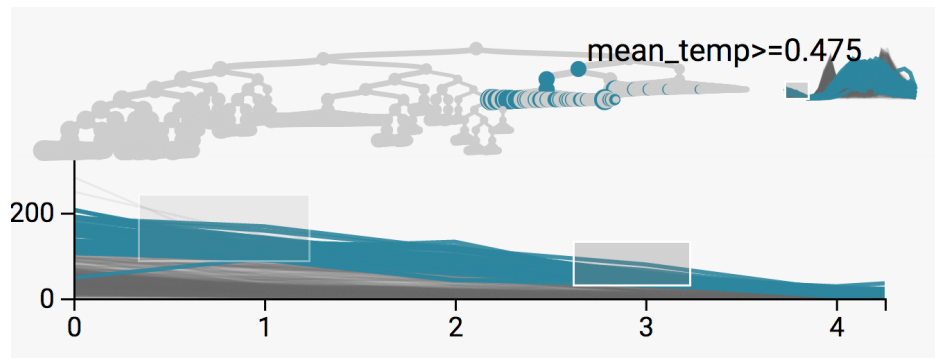


Figure 18: The samples with highest night demand tend to fall on warm weekends.

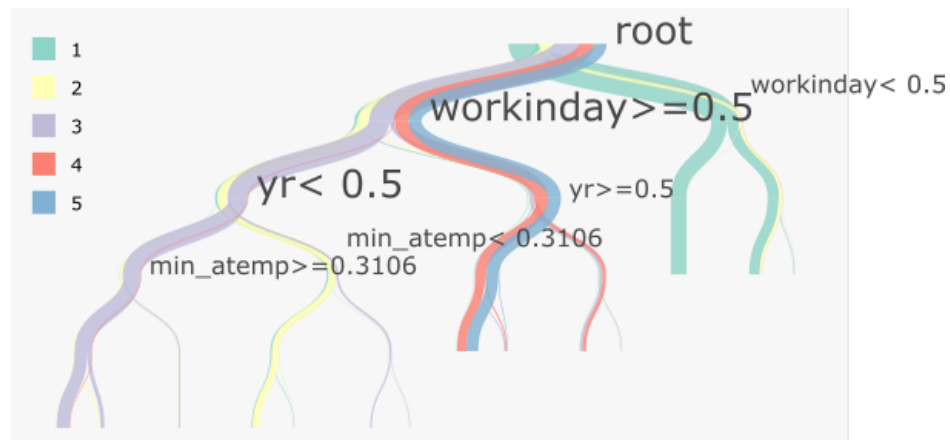


Figure 19: We can interpret the regression tree using an interactive DOI representation.

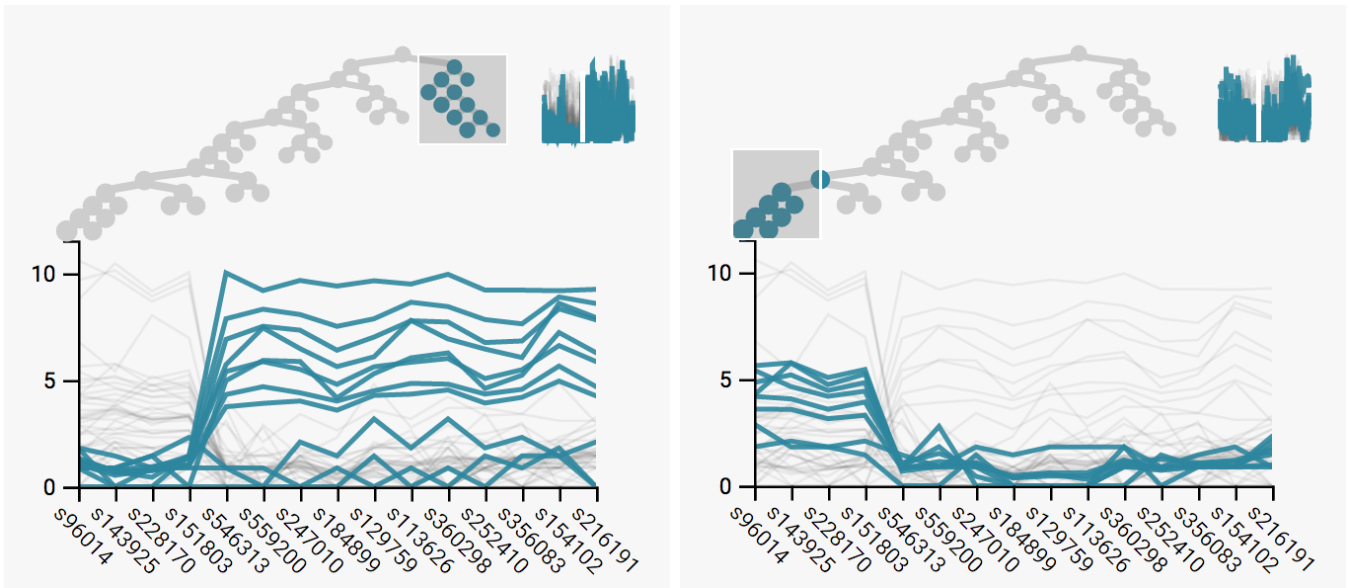


Figure 20: An application to the Global Patterns demonstrates how linking in treelapse can be applied to combine hierarchical clustering and parallel coordinates views.

0.4.5 Hierarchically Clustering the Global Patterns Data

Each of the timebox tree and treebox examples presented so far have focused on data with a clear time component. We note however that these techniques could alternatively be applied to high-dimensional data, via the use of parallel coordinates (Inselberg and Dimsdale 1991). The usual parallel coordinates challenges remain, namely selecting scales for and an ordering across the different coordinates, but the linking and focus-plus-context ideas can still be employed in this setting. Here we provide an implementation of this idea on a dataset comparing microbiomes across various ecological environments (Caporaso et al. 2011), which is publicly accessible through the phyloseq R package (McMurdie and Holmes 2013).

The original Global Patterns data consists of 26 samples across 9 environments (for example, freshwater and soil). In each site, there are counts across 19216 taxa – to simplify visualization, we filter to the 500 most abundant taxa.

We hierarchically cluster these 26 samples based on the 500 most abundant taxa, using complete linkage on the UniFrac distance. Figure 20 displays the resulting hierarchy together with a parallel coordinates view of the asinh transformed taxa.

In Figure 20, we compare two subclusters from the hierarchical clustering tree, after zooming to a few of the bacteria that distinguish between the clusters. Upon revisiting the original data, it becomes clear that the samples highlighted on the left come from freshwater samples, while those on the right come from soil and skin, and looking up taxonomic groups associated with the distinguishing bacteria confirms this. For example, many of the species with high abundances in the left figure come from order Oceanospirillales.

0.5 Conclusion and Future Work

Here, we have reviewed some fundamental principles of data visualization and described their implementation in a new treelapse package. Further, we have provided examples of the practical usefulness of these principles in real-world data analysis situations.

This package has only developed basic ideas, and there are a number of potentially useful extensions worth exploring. For example, we have not considered the principle of arrangement in our visualizations (Buja, Cook, and Swayne 1996), though many of our conclusions were based on comparing alternative selections of the same display. We could imagine faceting our displays across groups to make these types of comparisons more accessible. Further, we have only worked with the DOI distribution described in (Heer and Card 2004). It would be interesting to define a more statistical notion of interest along nodes, based on cognostics, for example (Hafen et al. 2013, J. H. Friedman and Stuetzle (2002)). A simple extension could be to allow graph layouts instead of trees in time and treebox displays, for data that cannot be coerced into a hierarchical structure. Finally, if these ideas turn out to be useful in practice, it would be valuable to modularize the basic visualization layouts and relationships into a library, allowing the wider community to construct novel linked, interactive graphics with minimal effort.

In summary, we have built an easily accessible R package for visualization techniques in a very specific methodology problem – analysis of differential abundance and dynamics in hierarchically structured data – that appears in a variety of application domains. We have leveraged a link between R and D3 (Vaidyanathan et al. 2014) to create visualizations during the exploratory phase of data analysis; in this way our work is a departure from the culture of polished, journalistic visualizations prioritized by the D3 community. Finally, we have given a series of examples to demonstrate how the general visualization techniques of focus-plus-context and linked brushing can be practically incorporated into a range of practical analysis workflows, from studying the impact of bacteria on human health to better allocating units in commuter bikesharing systems.

0.6 References

- Anders, Simon, and Wolfgang Huber. 2010. “Differential Expression Analysis for Sequence Count Data.” *Genome Biology* 11 (10). BioMed Central: 1.
- Becker, Richard A, and William S Cleveland. 1987. “Brushing Scatterplots.” *Technometrics* 29 (2). Taylor & Francis Group: 127–42.
- Boz, Olcay. 2002. “Extracting Decision Trees from Trained Neural Networks.” In *Proceedings of the Eighth*

- Breiman, Leo, Jerome Friedman, Charles J Stone, and Richard A Olshen. 1984. *Classification and Regression Trees*. CRC press.
- Brewer, Cynthia A, Geoffrey W Hatchard, and Mark A Harrower. 2003. “ColorBrewer in Print: A Catalog of Color Schemes for Maps.” *Cartography and Geographic Information Science* 30 (1). Taylor & Francis: 5–32.
- Buja, Andreas, Dianne Cook, and Deborah F Swayne. 1996. “Interactive High-Dimensional Data Visualization.” *Journal of Computational and Graphical Statistics* 5 (1). Taylor & Francis: 78–99.
- Caporaso, J. Gregory, Christian L Lauber, William A Walters, Donna Berg-Lyons, Catherine A Lozupone, Peter J Turnbaugh, Noah Fierer, and Rob Knight. 2011. “Global Patterns of 16S rRNA Diversity at a Depth of Millions of Sequences Per Sample.” *Proceedings of the National Academy of Sciences* 108 (Supplement 1). National Acad Sciences: 4516–22.
- Cho, Ilseung, and Martin J Blaser. 2012. “The Human Microbiome: At the Interface of Health and Disease.” *Nature Reviews Genetics* 13 (4). Nature Publishing Group: 260–70.
- Consortium, Human Microbiome Project, and others. 2012. “Structure, Function and Diversity of the Healthy Human Microbiome.” *Nature* 486 (7402). Nature Publishing Group: 207–14.
- Dethlefsen, Les, Sue Huse, Mitchell L Sogin, and David A Relman. 2008. “The Pervasive Effects of an Antibiotic on the Human Gut Microbiota, as Revealed by Deep 16S rRNA Sequencing.” *PLoS Biol* 6 (11). Public Library of Science: e280.
- DiGiulio, Daniel B, Benjamin J Callahan, Paul J McMurdie, Elizabeth K Costello, Deirdre J Lyell, Anna Robaczewska, Christine L Sun, et al. 2015. “Temporal and Spatial Variation of the Human Microbiota During Pregnancy.” *Proceedings of the National Academy of Sciences* 112 (35). National Acad Sciences: 11060–5.
- Friedman, Jerome H, and Werner Stuetzle. 2002. “John W. Tukey’s Work on Interactive Graphics.” *Annals of Statistics*. JSTOR, 1629–39.
- Hafen, Ryan, Luke Gosink, Jason McDermott, Karin Rodland, Kleese-Van Dam, William S Cleveland, and others. 2013. “Trelliscope: A System for Detailed Visualization in the Deep Analysis of Large Complex Data.” DTIC Document.
- Heer, Jeffrey, and Stuart K Card. 2004. “DOITrees Revisited: Scalable, Space-Constrained Visualization of Hierarchical Data.” In *Proceedings of the Working Conference on Advanced Visual Interfaces*, 421–24.

- Hochheiser, Harry, and Ben Shneiderman. 2004. “Dynamic Query Tools for Time Series Data Sets: Timebox Widgets for Interactive Exploration.” *Information Visualization* 3 (1). SAGE Publications: 1–18.
- Ihaka, Ross, and Robert Gentleman. 1996. “R: A Language for Data Analysis and Graphics.” *Journal of Computational and Graphical Statistics* 5 (3). Taylor & Francis: 299–314.
- Inselberg, Alfred, and Bernard Dimsdale. 1991. “Parallel Coordinates.” In *Human-Machine Interactive Systems*, 199–233. Springer.
- McMurdie, Paul J, and Susan Holmes. 2013. “Phyloseq: An R Package for Reproducible Interactive Analysis and Graphics of Microbiome Census Data.” *PloS One* 8 (4). Public Library of Science: e61217.
- Saito, Kazumi, and Ryohei Nakano. 2002. “Extracting Regression Rules from Neural Networks.” *Neural Networks* 15 (10). Elsevier: 1279–88.
- Swayne, Deborah F, Dianne Cook, and Andreas Buja. 1998. “XGobi: Interactive Dynamic Data Visualization in the X Window System.” *Journal of Computational and Graphical Statistics* 7 (1). Taylor & Francis Group: 113–30.
- Vaidyanathan, Ramnath, Joe Cheng, Joseph Allaire, Yihui Xie, and Kent Russell. 2014. “Htmlwidgets: HTML Widgets for R.” *R Package Version 0.3* 2.
- Willett, Wesley, Jeffrey Heer, and Maneesh Agrawala. 2007. “Scented Widgets: Improving Navigation Cues with Embedded Visualizations.” *IEEE Transactions on Visualization and Computer Graphics* 13 (6). IEEE: 1129–36.
- Xie, Yihui, Heike Hofmann, Di Cook, and Xiaoyue Cheng. 2013. “Cranvas: Interactive Statistical Graphics Based on Qt.” *R Package Version 0.8* 3.